ELSEVIER

Precambrian Research 116 (2002) 111–127

Precambrian Research

www.elsevier.com/locate/precamres

Svecofennian magmatic and metamorphic evolution in southwestern Finland as revealed by U-Pb zircon SIMS geochronology

Markku Väisänen [a,*], Irmeli Mänttäri [b], Pentti Hölttä [b]

[a] Department of Geology, University of Turku, FIN-20014 Turku, Finland
[b] Geological Survey of Finland, P.O. Box 96, FIN-02151 Espoo, Finland

Received 1 June 2001; accepted 8 February 2002

Abstract

Zircons from six samples collected from igneous and metamorphic rocks were dated using the NORDSIM ion microprobe, in order to investigate the tectonic evolution of the Palaeoproterozoic Svecofennian Orogen in southwestern Finland. These rocks represent pre-collisional, collisional and post-collisional stages of the orogeny. The ion microprobe results reveal two age groups of granodioritic–tonalitic rocks. The intrusions have different tectonic settings: the Orijärvi granodiorite represents pre-collisional 1.91–1.88 Ga island-arc-related magmatism and yielded an age of 1898 ± 9 Ma, whereas the collision-related Masku tonalite was dated at 1854 ± 18 Ma. The latter age accords with more accurate previous conventional zircon age data and constrains the emplacement age of collisional granitoids to ≈ 1.87 Ga. This is interpreted to reflect the collision between the Southern Svecofennian Arc Complex with the Central Svecofennian Arc complex and the formation of a suture zone between them during D2 deformation. Granulite facies metamorphism in the Turku area was dated at 1824 ± 5 Ma using zircons from leucosome in the Lemu metapelite. This age constrains D3 folding related to post-collisional crustal shortening in this area. Crustal melting continued until ≈ 1.81 Ga, as indicated by the youngest leucosome zircons and metamorphic rims of enderbite zircons. New metamorphic zircon growth took place in older granitoids at granulite facies, but not at amphibolite facies. Detrital zircons with ages between 2.91 and 1.97 Ga were found in the mesosome of the Lemu metapelite and 2.64–1.93 Ga inherited cores were found in the 1.87 Ga Masku tonalite.

Keywords: Svecofennian Orogen; Palaeoproterozoic; Ion microprobe; Tectonics; Crustal evolution

1. Introduction

Since the early pioneering works of Kouvo (1958), Wetherill et al. (1962) and Kouvo and Tilton (1966), the number of U-Pb datings on zircons has increased enormously in Finland (see e.g. Huhma, 1986; Patchett and Kouvo, 1986;

* Corresponding author. Fax: +358-2-3336-580.
E-mail addresses: markku.vaisanen@utu.fi (M. Väisänen), irmeli.manttari@gsf.fi (I. Mänttäri), pentti.holtta@gsf.fi (P. Hölttä).

0301-9268/02/$ - see front matter
PII: S0301-9268(02)00019-0

Vaasjoki, 1996), paving the way for a clearer understanding of the evolution of the Precambrian crust in the Fennoscandian shield. The ion microprobe studies have revealed that even a single zircon may have a multiple growth history, making the interpretation of conventional analyses difficult or even misleading in some cases. Although ion microprobe analyses are not quite as accurate as conventional analyses, the spatial resolution of ion microprobe is the only method capable of dating multiply grown domains in a single zircon (see Williams, 1998 for review). The recent works of Mezger and Krogstad (1997) and Lee et al. (1997) have shown that zircons can survive temperatures in excess of 900 °C without resetting the U-Pb system. This suggests that inherited, primary and metamorphic zircons of different ages can survive and be distinguished by ion microprobe.

In this work, we have attempted to constrain the temporal evolution of granitoid magmatism and high-grade metamorphism using the secondary ion mass spectrometer (SIMS) for selected samples collected in southwestern part of the Late Svecofennian Granite–Migmatite zone (LSGM, Fig. 1), which is a high temperature–low pressure amphibolite to granulite facies migmatite zone (Ehlers et al., 1993).

The aims of the study are:

(i) dating of the early (syn-)orogenic granitoids. The main questions regarding the granitoids in the LSGM are: (a) Are some of the plutonic rocks related to the island–arc volcanism in southern Finland? (b) Is the synorogenic magmatism younger in the LSGM than in the Tampere area north of the LSGM? (Fig. 1) (c) Are the previous conventional datings of synorogenic granitoids in the LSGM a mixture of magmatic zircons and younger metamorphic zircons and how much inherited zircons the granitoids contain?

(ii) dating of the granulite facies metamorphism.

(iii) dating of any possible metamorphism that predated the peak metamorphism.

(iv) dating of the deformation events. According to Väisänen and Hölttä (1999), high grade metamorphism in the LSGM took place syntectonically with D3 deformation that overprinted the synorogenic granitoids emplaced during D2 deformation. By dating anatectic leucosomes that are syntectonic with D3, we obtain the age of D3 as well. By dating synorogenic granitoids that are syntectonic with D2, we also know the age of this deformation.

For these purposes zircons from three granitoid samples, two leucosome samples and one mica gneiss sample were dated in this study.

2. Regional geology

The Svecofennian Orogen was formed by accretion of island arcs and ophiolites against the Archaean craton between 2.0 and 1.75 Ga (Gaál and Gorbatchev, 1987; Kontinen, 1987; Nironen, 1997). Collisional tectonics and possible magmatic underplating thickened the crust to its maximum thickness of 65 km in central Finland and <50 km in the LSGM (Korja et al., 1993), where the peak metamorphic conditions were reached later than in central Finland (Korsman et al., 1984). In the central Finland Granitoid Complex (CFGC; Fig. 1) regional metamorphism was coeval with the main phase of synorogenic magmatism at 1.89–1.88 Ga (Vaasjoki and Sakko, 1988; Haudenschild, 1995; Hölttä, 1995).

In the Tampere Schist Belt (TSB; Fig. 1) and in the CFGC the volcanic rock are dated at 1.90–1.89 Ga (Kähkönen et al., 1989), synorogenic granitoids are dated at 1.89–1.88 Ga (Nironen, 1989) while the 1.88–1.87 Ga granitoids are evidently post-kinematic (Nironen et al., 2000). Ages of volcanic and synorogenic rocks are, therefore, partly overlapping. The age of metamorphism is accurately determined in this area by conventional U-Pb dating of leucosome and mesosome monazites yielding a concordant age of 1878.5 ± 1.5 Ma (Mouri et al., 1999). This is coeval with the synorogenic magmatism in that area (Nironen, 1989).

In the LSGM, the previous conventional datings of the synorogenic granitoids span between 1.90 and 1.87 Ga (Hopgood et al., 1983; Huhma, 1986; Patchett and Kouvo, 1986) but most cluster around 1.87 Ga (Patchett and Kouvo, 1986; Van

Duin, 1992; Nironen, 1999). The magmatism dated at ≈ 1.87 Ga is syntectonic in relation to deformation (Väisänen and Hölttä, 1999). In the eastern part of the LSGM (≈ 400 km east from the present study area), zircons from leucosomes and mesosomes yielded ages between 1850 and 1800 Ma (Korsman et al., 1984). Considering the possible inheritance and large uncertainties in previous datings, the age of peak metamorphism has remained unclear. Anatectic granites in the LSGM are dated at ≈ 1840–1810 Ma (Huhma, 1986; Suominen, 1991; Väisänen et al., 2000).

On the basis of these age determinations, high temperature metamorphism (≈ 800 °C/4–6 kbars) culminated in the LSGM during the late orogenic or post-collisional stage of the Svecofennian Orogen between 1840 and 1810 Ma. It overprinted and, in places, effectively obscured the earlier features of the orogeny (Korsman et al., 1984; Schreurs and Westra, 1986; Väisänen and

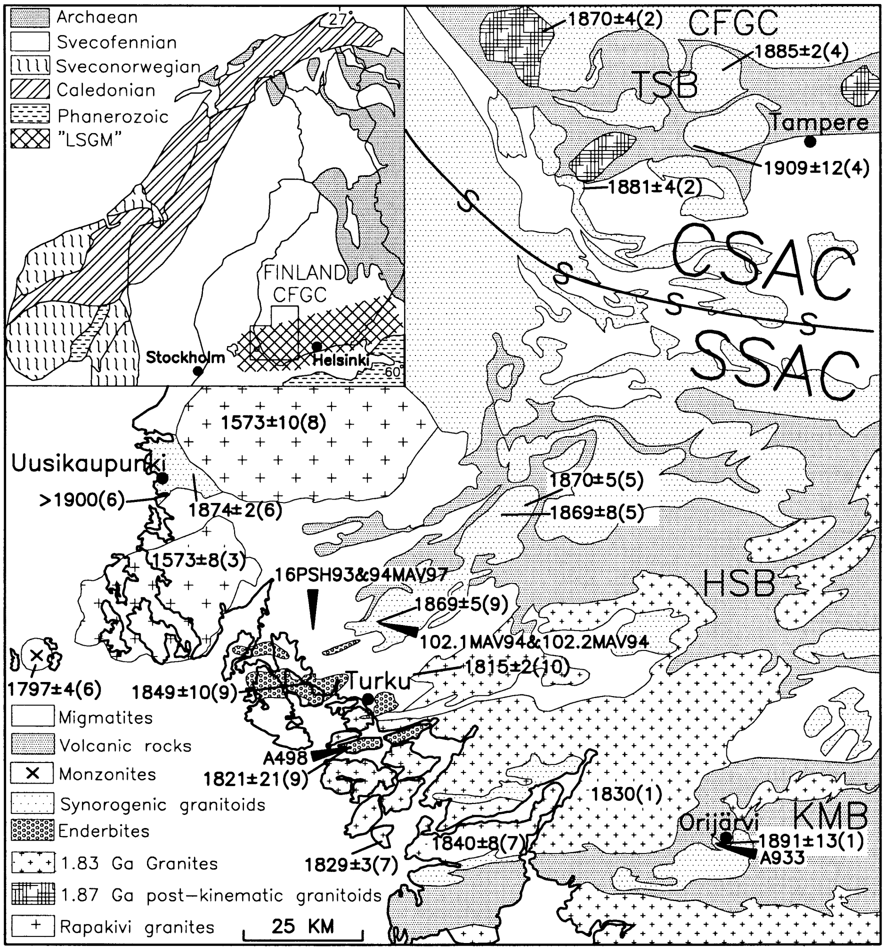

Fig. 1. Main lithological units of SW Finland. Some of the conventional U-Pb zircon ages of granitoids are numbered: (1) = Huhma (1986), (2) = Kilpeläinen (1998), (3) = Lindberg and Bergman (1993), (4) = Nironen (1989), (5) = Nironen (1999), (6) = Patchett and Kouvo (1986), (7) = Suominen (1991), (8) = Vaasjoki (1977), (9) = Van Duin (1992), (10) = Väisänen et al. (2000). Sample locations in this study are shown by black arrows. CFGC, Central Finland Granitoid Complex; CSAC, Central Svecofennian Arc Complex; HSB, Häme Schist Belt; KMB, Kemiö–Mäntsälä Belt; LSGM, Late Svecofennian Granite–Migmatite zone; SSAC, Southern Svecofennian Arc Complex; TSB, Tampere Schist Belt. Solid line marked by 'S' is approximate location of suture zone proposed by Lahtinen (1996). Map compiled after Hietanen (1947), Kilpeläinen (1998) and Korsman et al. (1997).

Hölttä, 1999; Väisänen et al., 2000). Only relatively small areas, such as that of the Orijärvi area, remained unmagmatized. Because of the high heat flow, zircons in pre-granulite facies rocks might have been affected by this late metamorphism, as suggested by the very heterogeneous zircon age data on enderbites in the Turku granulite area (Suominen, 1991; Van Duin, 1992; Fig. 1).

In the LSGM, high grade metamorphism and late orogenic S-type granites at 1.84–1.81 Ga are interpreted to be related to post-collisional mafic intraplating (Väisänen et al., 2000). An exception to this is the western part of the volcanic Kemiö–Mäntsälä Belt (west of Orijärvi in Fig. 1), where metamorphism did not reach melting conditions and was probably related to earlier orogenic stage (e.g. Ploegsma and Westra, 1990). Post-collisional ≈ 1.80 Ga shoshonitic intrusions (Eklund et al., 1998) and ≈ 1.60 Ga rapakivi granites (Vaasjoki, 1977) represent the latest magmatic events (Fig. 1).

Deformation in the LSGM is attributed to at least two main stages. The first stage was the collision of the Southern Svecofennian Arc Complex with the Central Svecofennian Arc Complex during D2 north-vergent thrusting and intrusion of synorogenic granitoids. This produced a suture zone between the two arc complexes. The second stage involved continued crustal convergence producing the main regional, upright, E–W trending D3 folds simultaneously with crustal anatexis and the formation of migmatites and granites (Lahtinen, 1994; Korsman et al., 1999; Väisänen and Hölttä, 1999; Fig. 1).

3. Sample descriptions

The six samples chosen for SIMS analyses are described below. The sampling locations are displayed in Fig. 1.

3.1. A933: Orijärvi granodiorite

The Orijärvi granodiorite is a composite batholith ranging in composition from gabbro to tonalite with minor hornblendites and granodiorites (sample A933 in this study, Fig. 1). It was chosen for dating for two reasons. Firstly, previous conventional U-Pb dating of the granodiorite at 1891 ± 13 Ma (Huhma, 1986) did not unambiguously distinguish between volcanic versus orogenic origin of the batholith because of large uncertainties. Secondly, regional metamorphism in this area is of andalusite–cordierite grade (Schreurs and Westra, 1986). This is the lowest in southern Finland. On this basis, the metamorphic imprint on zircons should be absent allowing comparison for the other samples from the higher grade Turku area. The rock is medium- to coarse-grained, weakly foliated and contains mafic enclaves. This sample is the same used by Huhma (1986). National grid coordinates are 6678800–2474700.

3.2. 102.1MV94: Masku tonalite

The hornblende–tonalite sample from Masku was collected from the same locality as the sample dated at 1869 ± 5 Ma by Van Duin (1992). The reason for choosing this sample was to check if there is any metamorphic overprint on the zircons. The outcrop is situated on the transitional granulite–amphibolite facies boundary. The rock contains mafic enclaves and shows a weak D2 fabric (Väisänen and Hölttä, 1999). National grid coordinates are 6719150–1567550.

3.3. A498: Kakskerta enderbite

The sample is from medium- to coarse-grained orthopyroxene bearing enderbite from Kakskerta, Turku. The rock type has been previously described as charnockite by Hietanen (1947), pyroxene granodiorite by Suominen (1991) and leuconorite by Van Duin (1992). Two conventional U-Pb zircon datings have been carried out on the same intrusion. Suominen (1991) concluded that his sample yielded an age interval of 1842–1879 Ma with probably two zircon generations and Van Duin (1992) obtained an age of 1821 ± 39 Ma. On the structural basis, however, the rock belongs to the early orogenic group showing the D2 fabric (Väisänen and Hölttä, 1999) suggesting that substantial metamorphic zircon growth has occurred. The sample used in this study is the same used by Suominen (1991). National grid coordinates are 6694370–1565120.

3.4. 102.2MAV94: leucosome in the Masku tonalite

This sample is collected from the same exposure as the sample 102.1MAV94. The sample is a pink granitic leucosome in the hornblende–tonalite host. It occurs as patches and heterogeneous veins cutting the D2 fabric. The reason for sampling was to date the age of leucosome formation.

3.5. 16PSH93: leucosome of the Lemu garnet–cordierite gneiss

The sample is collected from garnet- and cordierite-bearing granitic leucosome from the low P-high T garnet-cordierite gneiss of Lemu. The sample is taken from the hinge of a subhorizontal, E–W trending F3 fold where the leucosome intrudes its the axial plane. The amount of leucosome is about 50% at this locality. The reason for sampling was to date the age of leucosome formation. National grid coordinates are 6716100–1552700.

3.6. 94MAV97: mesosome of the Lemu garnet-cordierite gneiss

The sample is from mesosome of the low P–high T migmatite, Lemu. The mesosome is biotite-rich and contains garnet and cordierite porphyroblasts. The texture is distinctly foliated and segregated with millimeter-scale alternating dark and light bands parallel to foliation. Leucosome, represented by the light bands could not be avoided. The purpose of this sample was to date detrital and metamorphic zircons. National grid coordinates are 6714750–1551850.

4. Analytical methods

The ion microprobe analyses were run at the NORDSIM laboratory using the Cameca IMS 1270 secondary ion mass spectrometer (SIMS) located at the Swedish Museum of Natural History, Stockholm. The spot diameter for the 4nA primary O_{2-} ion beam was ≈ 30 μm and oxygen flooding in the sample chamber was used to increase the production of Pb^+ ions. Four counting blocks comprising a total of twelve cycles of the Pb, Th and U species were measured at each spot. The mass resolution was (M/ΔM) of 5400 (10%). The raw data were calibrated against a zircon standard (91,500; Wiedenbeck et al., 1995) and corrected for background (204.2) and modern common lead ($T = 0$; Stacey and Kramers, 1975). For further details of the analytical procedures see Whitehouse et al. (1997, 1999). The plotting of the U-Pb data, the fitting of the discordia lines and the calculation of the concordia intercept ages were carried out using the Isoplot/Ex program (Ludvig, 1998).

5. Results

Ion microprobe isotope analyses for respective samples are presented in Table 1 and Fig. 2 illustrates the back-scattered electrons (BSE) images of selected zircon crystals. Analytical uncertainties in the text and in the concordia diagrams are presented with 2σ errors. Summary of the results is presented in Table 2.

5.1. A933: Orijärvi granodiorite

Zircons from the Orijärvi granodiorite are typical magmatic zircons with euhedral elongated prismatic shapes (100–250 μm, length/width ratios between 5:1 and 2:1) and clear magmatic zoning (Fig. 2a). Generally, the zircons are colourless and transparent, but a few have turbid core domains. In BSE images presumably older cores are visible in a few zircons (Fig. 2b).

A total of 13 spots were analysed using the ion microprobe. The U and Pb concentrations are moderate and vary in a reasonable range, except for very high U, Th and Pb concentrations in the inner domain of zircon 16. Most of the age data plot on a discordia line with an upper intercept age of 1889 ± 11 Ma (MSWD = 2.9; $n = 12$). Outside this line plots analysis number n207–17b.

Table 1
Ion microprobe U-Pb data on zircons

Sample/ spot No.	Analyzed zircon domain[d]	Derived ages[a]						Corrected ratios[a]						Elemental data						
		$^{207}Pb/^{206}Pb$	±s	$^{207}Pb/^{235}U$	±s	$^{206}Pb/^{238}U$	±s	$^{207}Pb/^{206}Pb$	±s (%)	$^{207}Pb/^{235}U$	±s (%)	$^{206}Pb/^{238}U$	±s (%)	Rho[b]	Disc.[c] (%)	(U) ppm	(Th) ppm	(Pb) ppm	Th/U meas.	$^{206}Pb/^{204}Pb$ meas.
A933, Orijärvi granodiorite																				
n671-01a	Zoned	1907	8	1897	18	1887	33	0.1168	0.4	5.475	2.1	0.3400	2.0	0.98		327	87	132	0.27	2.55E+04
n671-07a	Zoned	1889	10	1967	19	2042	36	0.1156	0.6	5.939	2.1	0.3727	2.0	0.97	−4.3	263	63	116	0.24	4.07E+04
n671-12a	Zoned	1915	10	1910	18	1905	34	0.1172	0.6	5.559	2.1	0.3439	2.0	0.96		214	83	90	0.39	7.67E+03
n671-17b	Homog-core	1890	11	1903	18	1915	34	0.1157	0.6	5.516	2.1	0.3458	2.0	0.96		301	70	124	0.23	4.06E+04
n671-22a	Zoned-inner	1857	11	1750	18	1662	30	0.1136	0.6	4.606	2.1	0.2941	2.1	0.96	7.4	171	44	60	0.26	6.64E+03
n671-22b	Zoned-outer	1877	8	1907	18	1935	34	0.1148	0.5	5.542	2.1	0.3501	2.0	0.98		246	56	102	0.23	3.56E+04
n671-25a	Zoned	1874	9	1932	18	1987	35	0.1146	0.5	5.705	2.1	0.3611	2.0	0.97	−2.1	235	52	100	0.22	5.07E+04
n671-26a	Zoned-inner	1885	6	1923	18	1957	35	0.1154	0.3	5.642	2.1	0.3547	2.1	0.99		537	204	232	0.38	5.58E+04
n671-26b	Zoned-outer	1904	8	1945	18	1984	35	0.1165	0.4	5.792	2.1	0.3604	2.0	0.98	−0.2	237	54	101	0.23	2.98E+04
n207-16a	Zoned-inner	1866	4	1748	11	1650	19	0.1141	0.2	4.590	1.3	0.2917	1.3	0.98	11	3284	2742	1295	0.83	7.84E+04
n207-16b	Zoned-outer	1863	48	1618	28	1436	29	0.1139	2.7	3.919	3.5	0.2496	2.2	0.64	22	348	64	103	0.18	1.50E+04
n207-17a	Zoned-rim	1907	9	1907	14	1907	25	0.1167	0.5	5.542	1.6	0.3443	1.5	0.95		430	253	192	0.59	5.03E+04
n207-17b	Zoned-rim	1704	26	1533	14	1413	21	0.1044	1.4	3.528	1.8	0.2451	1.7	0.94	16	551	112	164	0.20	6.50E+02
102.1MAV94, tonalite																				
n673-02a	Homog-core	1925	26	1903	22	1882	34	0.1179	1.5	5.513	2.5	0.3391	2.1	0.81		147	58	63	0.39	4.78E+02
n673-17a	Zoned-inner	1873	11	1889	18	1903	34	0.1146	0.6	5.425	2.1	0.3435	2.0	0.96		278	123	118	0.44	3.96E+04
n673-20a	Zoned-core	1966	5	2021	19	2074	38	0.1207	0.3	6.317	2.1	0.3796	2.1	0.99	−1.8	914	17	391	0.02	1.87E+04
n201-07a	Zoned-outer	1859	8	1781	28	1716	51	0.1137	0.5	4.780	3.4	0.3049	3.4	0.99	3	312	123	118	0.39	1.12E+04
n201-07b	Zoned-inner	1841	5	1807	6	1777	10	0.1126	0.3	4.927	0.7	0.3174	0.6	0.96	3	1167	178	431	0.15	7.01E+03
n201-13a	Core	2635	7	2612	30	2582	67	0.1781	0.4	12.099	3.2	0.4927	3.1	0.99		120	86	82	0.72	3.16E+04
n201-13b	Rim	1859	4	1770	16	1695	29	0.1137	0.2	4.714	2.0	0.3008	1.9	0.99	7	820	89	283	0.11	2.52E+04
n201-20a	Zoned-core	1963	4	2051	51	2139	105	0.1205	0.2	6.535	5.8	0.3934	5.8	1.00		501	401	334	0.80	1.04E+05

Table 1 *(continued)*

Sample/ spot No.	Analyzed zircon domain[d]	Derived ages[a]						Corrected ratios[a]						Elemental data						
		$^{207}Pb/^{206}Pb$	±s	$^{207}Pb/^{235}U$	±s	$^{206}Pb/^{238}U$	±s	$^{207}Pb/^{206}Pb$	±s (%)	$^{207}Pb/^{235}U$	±s (%)	$^{206}Pb/^{238}U$	±s (%)	Rho[b]	Disc.[c] (%)	(U) ppm	(Th) ppm	(Pb) ppm	Th/U meas.	$^{206}Pb/^{204}Pb$ meas.
n201-20b	Zoned-outer	1716	10	1218	5	957	6	0.1051	0.6	2.319	0.8	0.1600	0.6	0.82	47	1736	665	339	0.38	2.48E+03
102.2MAV94, leucosome in Masku tonalite																				
n199-23a	Core	1891	7	1833	12	1783	21	0.1157	0.4	5.083	1.4	0.3186	1.3	0.96	4	324	108	125	0.33	1.58E+05
n199-23b	Zoned-rim	1810	2	1809	7	1807	14	0.1106	0.1	4.937	0.9	0.3236	0.9	0.99		2456	135	895	0.05	2.25E+05
n199-24a	Homog-core	1793	4	1771	9	1753	16	0.1096	0.2	4.721	1.1	0.3125	1.0	0.98	1	1026	34	359	0.03	1.19E+05
n199-28b	Homog-core	1876	7	1848	13	1824	24	0.1147	0.4	5.174	1.6	0.3270	1.5	0.97	0	257	101	103	0.39	2.19E+05
n199-28c	Rim	1793	3	1757	11	1728	20	0.1096	0.2	4.645	1.3	0.3074	1.3	0.99	2	2475	112	855	0.05	1.17E+05
n199-29a	Homog-core	1803	4	1785	11	1769	21	0.1102	0.2	4.800	1.3	0.3158	1.3	0.99		1221	91	436	0.07	2.56E+05
n199-29b	Homog-rim	1795	3	1760	10	1730	18	0.1097	0.2	4.657	1.2	0.3078	1.2	0.99	2	2104	105	728	0.05	1.88E+05
n199-31a	Core	1842	6	1769	18	1708	31	0.1126	0.3	4.712	2.1	0.3034	2.1	0.99	4	381	64	135	0.17	1.75E+04
n199-31b	Rim	1800	5	1725	6	1663	10	0.1101	0.3	4.467	0.7	0.2944	0.7	0.94	7	1537	64	509	0.04	1.84E+04
A498, Kakskerta enderbite																				
n672-05a	Zoned-core	1868	5	1874	18	1879	34	0.1143	0.3	5.330	2.1	0.3383	2.1	0.99		790	136	310	0.17	3.95E+04
n672-09a	Homog-core	1761	13	1816	18	1864	33	0.1077	0.7	4.978	2.2	0.3353	2.0	0.94	−1.2	283	126	114	0.44	1.51E+03
n672-09b	Homog-rim	1885	7	1861	18	1840	34	0.1153	0.4	5.253	2.1	0.3304	2.1	0.99		1589	67	591	0.04	4.68E+03
n672-14a	Zoned-core	1889	7	1913	18	1936	35	0.1156	0.4	5.582	2.1	0.3502	2.1	0.98		295	144	129	0.49	1.16E+05
n672-21a	Homog-core	1849	5	1862	18	1873	34	0.1131	0.3	5.256	2.1	0.3372	2.1	0.99		1540	170	593	0.11	5.43E+04
n672-21b	Homog-rim	1866	8	1828	35	1795	63	0.1141	0.5	5.052	4.0	0.3211	4.0	0.99		2097	48	753	0.02	4.44E+04
n672-26a	Zoned-rim	1816	10	1825	18	1834	33	0.1110	0.6	5.036	2.1	0.3291	2.0	0.97		331	175	137	0.53	6.75E+03
n203-02a	Zoned-core	1866	7	1778	31	1703	56	0.1141	0.4	4.758	3.7	0.3023	3.7	0.99	3	623	67	217	0.11	1.28E+04
n203-02b	Homog-rim	1753	11	1720	46	1693	81	0.1072	0.6	4.439	5.5	0.3003	5.5	1.00		2147	94	725	0.04	9.89E+03
n205-10a	Homog-core	1842	11	1850	12	1857	22	0.1126	0.6	5.183	1.4	0.3339	1.3	0.93		1833	216	705	0.12	7.1IE+03

Table 1 *(continued)*

Sample/ spot No.	Analyzed zircon domain[d]	Derived ages[a]						Corrected ratios[a]						Elemental data						
		$^{207}Pb/^{206}Pb$	±s	$^{207}Pb/^{235}U$	±s	$^{206}Pb/^{238}U$	±s	$^{207}Pb/^{206}Pb$	±s (%)	$^{207}Pb/^{235}U$	±s (%)	$^{206}Pb/^{238}U$	±s (%)	Rho[b]	Disc.[c] (%)	(U) ppm	(Th) ppm	(Pb) ppm	Th/U meas.	$^{206}Pb/^{204}Pb$ meas.
n205-24a	Homog-core	1859	3	1910	9	1957	18	0.1137	0.2	5.559	1.1	0.3546	1.1	0.98	-4	1719	519	729	0.30	6.87E+04
n205-24b	Homog-rim	1876	3	1879	6	1881	11	0.1148	0.2	5.361	0.7	0.3388	0.7	0.98		1947	14	739	0.01	1.81E+04
n205-27a	Zoned-core/inner	1834	7	1786	14	1745	25	0.1121	0.4	4.807	1.7	0.3109	1.7	0.98	2	1735	298	628	0.17	9.21E+03
n205-27b	Zoned-rim/outer	1818	7	1833	8	1847	15	0.1111	0.4	5.083	1.0	0.3318	0.9	0.98		806	62	316	0.08	1.02E+03
n206-04a	Homo -core	1837	4	1858	12	1877	22	0.1123	0.2	5.235	1.4	0.3380	1.3	0.99		1295	50	494	0.04	9.19E+03
16PSH93, Leucosome in Lemu garnet-cordierite gneiss																				
n674-20a	Homog-inner	1815	5	1836	18	1854	33	0.1109	0.2	5.096	2.1	0.3332	2.0	0.99		1125	25	418	0.02	5.15E+04
n198-03a	Homog-inner	1827	3	1813	10	1802	19	0.1117	0.2	4.964	1.2	0.3224	1.2	0.99		1055	24	381	0.02	3.30E+05
n198-03b	Homog-outer	1823	6	1816	17	1810	31	0.1114	0.3	4.981	2.0	0.3242	2.0	0.99		830	21	305	0.03	2.97E+03
n198-07b	Homog-outer	2556	49	2232	13	1895	21	0.1699	2.9	8.006	1.4	0.3418	1.3	0.92	28	1158	22	915	0.02	5.OOE+01
n198-08a	Zoned	1818	4	1827	58	1834	109	0.1111	0.2	5.043	6.8	0.3291	6.8	1.00		963	13	353	0.01	1.58E+05
n198-13b	Homog-rim	1820	53	1694	18	1594	26	0.1112	2.9	4.303	2.2	0.2806	1.8	0.83	11	795	18	292	0.02	2.60E+02
n200-06a	Homog-outer	1829	3	1841	9	1852	17	0.1118	0.1	5.130	1.1	0.3327	1.1	0.99		1777	11	659	0.01	3.57E+04
n204-24a	Homo-inner	1818	10	1760	19	1712	33	0.1111	0.5	4.658	2.3	0.3041	2.2	0.97	3	772	23	263	0.03	4.64E+04
94MAV97, Mesosome in Lemu garnet-cordierite gneiss																				
n200-0la	Zoned-core	2912	8	2798	20	2642	44	0.2108	0.5	14.724	2.1	0.5066	2.0	0.98	8	95	45	67	0.47	1.52E+03
n200-0lb	Homog-rim	2384	6	2260	8	2126	16	0.1534	0.4	8.261	0.9	0.3906	0.9	0.93	11	492	40	227	0.08	7.08E+03
n200-06a	Zoned	1829	3	1841	9	1852	17	0.1118	0.1	5.130	1.1	0.3327	1.1	0.99		1777	11	659	0.01	3.57E+04
n200-l0a	Homog-core	1977	2	1995	14	2013	28	0.1214	0.1	6.134	1.7	0.3664	1.6	1.00		2654	70	1099	0.03	7.10E+04
n200-l0c	Zoned-rim	1969	8	1889	18	1817	32	0.1208	0.4	5.424	2.1	0.3255	2.0	0.98	5	223	102	90	0.46	1.74E+04

[a] Errors are at 1 σ level.
[b] Rho, error correlation for $^{207}Pb/^{235}U$ versus $^{206}Pb/^{238}U$ ratios.
[c] Degree of discordance is calculated at the closest 2 σ limit.
[d] Core/rim, clear core domain with clear younger zircon phase. Inner/outer, most probably same zircon phase with analyses on center or border domains. Homog, guite homogeneous internal structure.

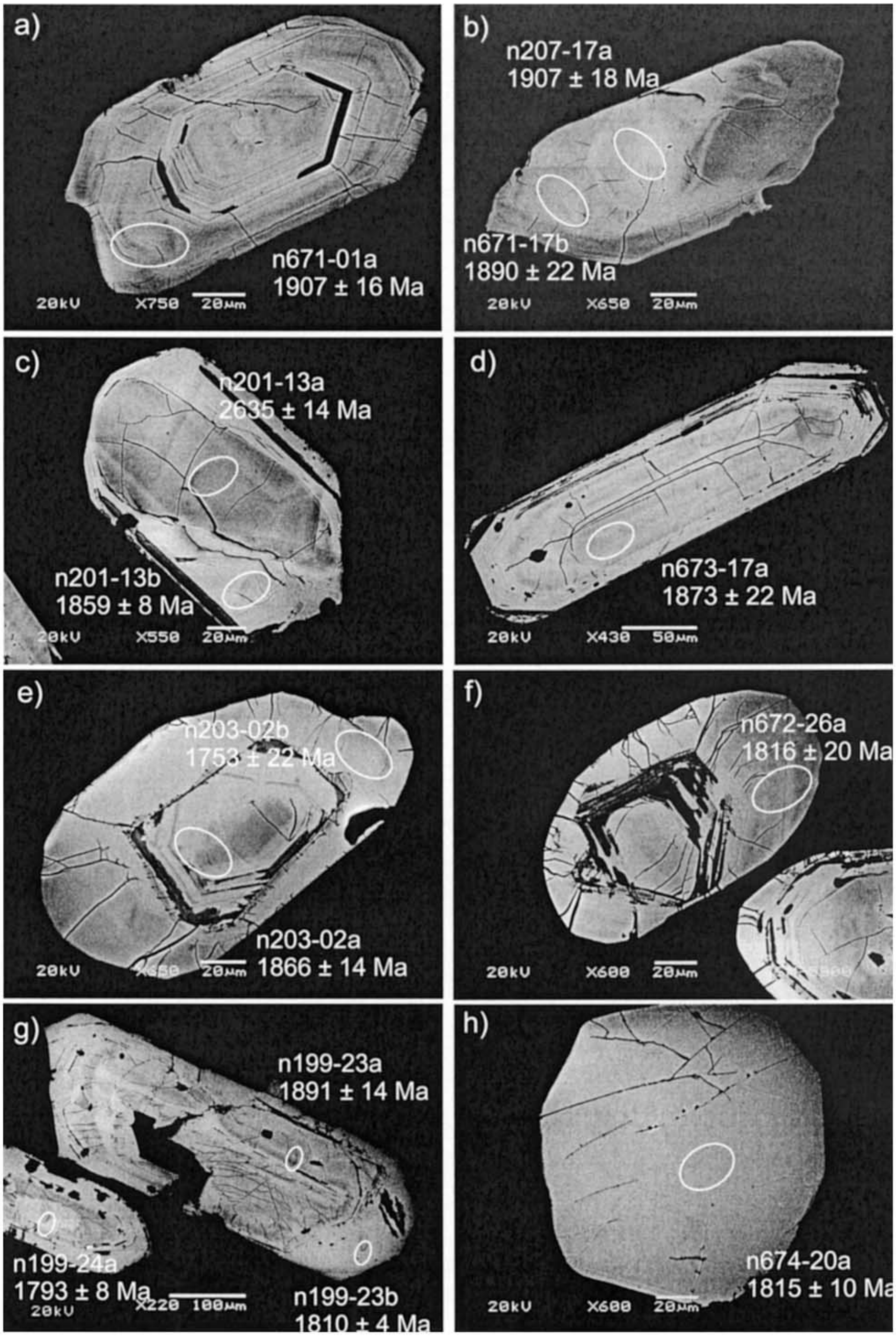

Fig. 2. BSE images of selected zircons. Sites of the spot analyses and corresponding $^{207}Pb/^{206}Pb$ ages (2σ) are marked on the figures. (a, b) A933 Orijärvi granodiorite; (c, d) 102.1MAV94 Masku tonalite; (e, f) A498 Kakskerta enderbite; (g) 102.2MAV94 Masku tonalite leucosome; (h) 16PSH93 Lemu garnet–cordierite gneiss leucosome.

Table 2
Summary of previous conventional and new SIMS data

Sample ID	Rock type	Previous conventional ID-TIMS age and Refs.	Ion microprobe U-Pb ages; this study			
			Analyzed zircon types/domains	n	Process	Apparent age
A933 Orijärvi	Granodiorite	1891 ± 13 Ma (Huhma, 1986)	Prismatic/zoned	12/13	Igneous age	Upper intercept age 1889 ± 11 Ma
			Prismatic/zoned	7/13	Igneous age	Concordia age 1898 ± 9 Ma
102.1MAV94 Masku	Tonalite	1869 ± 5 Ma (Van Duin, 1992)	Prismatic/zoned and rim domains	4/9	Igneous age	Upper intercept age 1866 ± 21 Ma
			Prismatic/zoned and rim domains	4/9	Igneous age	Weighted average age 1854 ± 18 Ma
			Cores	5/9	Inherited material	Archaean and older Palaeoproterozoic
A498 Kakskerta	Enderbite	1879–1842 Ma (Suominen, 1991) 1821 ± 39 Ma (Van Duin, 1992)	Zoned cores	4	Igneous age	Upper intercept age 1874 ± 56 Ma
			Homogeneous cores	4	Recrystallization	Upper intercept age 1804 ± 31 Ma
			Zoned rims	2	New zircon growth	Concordia age 1819 ± 7 Ma
			Homogeneous rims	3	Recrystallization/new zircon growth	Concordia age 1876 ± 5 Ma
			Homogeneous core + rim	2		$^{207}Pb/^{206}Pb$ ages ≈ 1.76 Ga
			Stubby/homogeneous rims and zoned cores	7/15	Igneous age?	Upper intercept age 1878 ± 19 Ma
			Stubby/homogeneous cores and zoned rims	6/15	Metamorphism?	Upper intercept age 1804 ± 31 Ma
102.2MAV94 Masku	Tonalite, leucosome		Prismatic/border domains (4) + homog.cores (2)	6/9	Leucosome crystallization	Upper intercept age1804 ± 14 Ma
			Prismatic/core domains	3/9	Older cores	Roughly equivalent with igneous age
16PSH93 Lemu	Garnet–cordierite gneiss, leucosome		Equidimensional, homogeneous and one zoned elongated (see text)	8/7	Age for migmatization	Weighted average age: 1826 ± 5 Ma
				6/7		Concordia age 1824 ± 5 Ma
94MAV97 Lemu	Garnet–cordierite gneiss, mesosome		Heterogeneous zircon material	4/5	Sedimentary zircons	Archaean and older Palaeoproterozoic

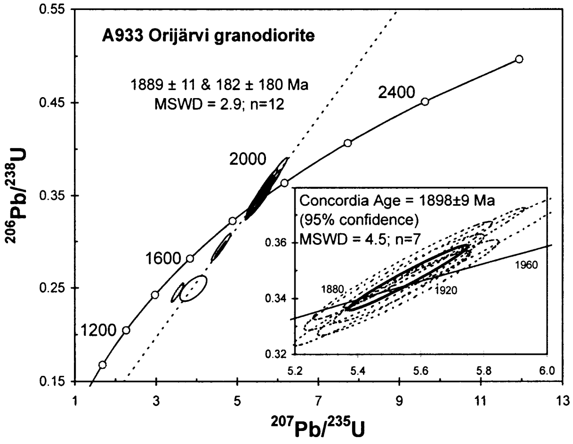

Fig. 3. Concordia plot for sample A933 Orijärvi granodiorite.

The fact that this particular analysis is strongly discordant and has $^{206}Pb/^{204}Pb$ ratio clearly lower than the second analytical attempt on the same zircon domain indicates that the first, discordant analyse was probably on a fissure. Because the age data forms a cluster on the concordia curve, the intercept age can also be calculated as a concordia age of 1898 ± 9 Ma (MSWD = 4.5; $n =$ 7) defined by seven concordant data points (Fig. 3).

5.2. 102.1MAV94: Masku tonalite

Zircons from the Masku tonalite are almost colorless and transparent. They are euhedral prismatic crystals with sharp surface angles and bipyramidal edges (200–350 μm long, length/width ratios between 5:1 and 2:1). Their internal structure seen in BSE-images is zoned and occasionally older cores and small nucleus are found (Fig. 2c,d).

Nine zircon spots were dated using the ion microprobe. Except for one rather discordant data point, the others are concordant or show only slight discordance. The U-Pb age data can be divided into two groups according to analyzed domains of the zircons. Ages from zoned zircons and border domains of zircons with cores plot roughly on a line with an upper intercept age of 1866 ± 21 Ma (MSWD = 7.4). When excluding the discordant point the upper intercept age is 1865 ± 47 Ma (MSWD = 7.3). We also calculated the weighted average of the $^{207}Pb/^{206}Pb$ ages from the four most concordant data points. The resulting age is 1854 ± 18 Ma. (95% C.I., MSWD = 4.1). These ages, the same within errors, are considered to reflect the time of emplacement of the Masku tonalite. The other four analyses from the core domains give clearly older Palaeoproterozoic and Archaean $^{207}Pb/^{206}Pb$ ages (Table 1 and Fig. 4).

5.3. A498: Kakskerta enderbite

Zircons from the Kakskerta enderbite are slightly elongate to stubby crystals (100–200 μm long, length/width ratios between 2:1 and 1:1) with partly smooth surfaces. The zircons have brown inner domains surrounded by colourless transparent rims. In BSE images (Fig. 2e,f), the inner domains and often fractured outer rims are separated by fractures which are filled with an unknown material.

A total of 15 zircon spots were dated using the ion microprobe. On the concordia diagram the U-Pb data scatter between 1.9 and 1.8 Ga. Four analyses from the magmatically zoned core domains give an upper intercept age of 1874 ± 56 Ma and four analyses from the homogenous core domains give an upper intercept age of 1804 ± 31

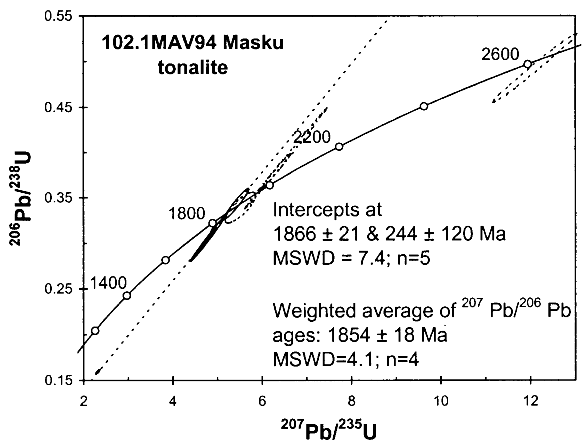

Fig. 4. Concordia plot for sample 102.1MAV94 Masku tonalite. Solid lines prismatic zoned zircons and rims, dashed lines inherited cores.

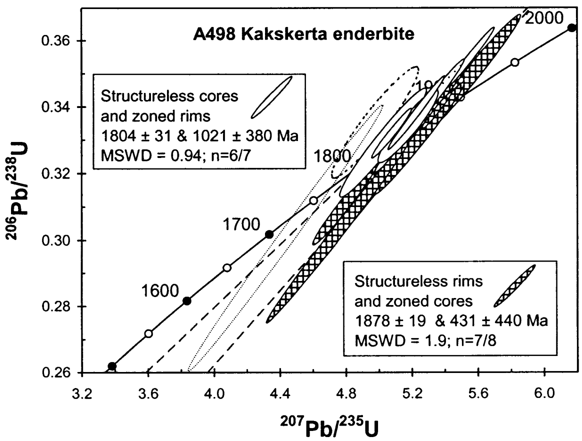

Fig. 5. Concordia plot for sample A498 Kakskerta enderbite.

Ma (MSWD = 0.94). The three dated structureless rim domains give a concordia age of 1876 ± 5 Ma and the two zoned rims have an approximate age of 1.82 Ga. Although this age data is difficult to interpret, it is suggested that the ages from the zoned core domains reflect the time of enderbite crystallization. In addition, the three homogeneous rim domains either recrystallized or grew during the enderbite crystallization. Then, the resulting age for the Kakskerta enderbite is 1878 ± 19 Ma (MSWD = 1.9). The ages from the internally homogeneous core domains must then reflect a later recrystallization of some older cores and the ages from zoned rim domains new zircon growth on some older grains. The age for the subsequent metamorphism can then be approximated at 1804 ± 31 Ma (Fig. 5).

5.4. 102.2MAV94: leucosome of the Masku tonalite

Zircons from the leucosome of the Masku tonalite are prismatic with sharp surface angles and bipyramidal edges. They are 100–200 μm long with length/width ratios between 5:1 and 2:1. Under a stereomicroscope, the colorless inner domains are enveloped by brown, translucent zircon material. In BSE images, the zircons are highly fractured and show structurally more homogeneous outer rim domains (Fig. 2g).

Nine zircon spots were dated using the ion microprobe. The ion microprobe ages from three core domains indicate roughly similar ages as the age of the Masku tonalite. All the four dated rim growths as well as two structurally homogeneous core domains give meaningfully younger ages, the upper intercept age being 1804 ± 14 Ma (MSWD = 0.94; Fig. 6). This is interpreted as the age of the leucosome crystallization. It is noteworthy that the zircon phase crystallized during the leucosome formation is rich in uranium and the Th/U-ratios are clearly lower compared to the other tonalite zircon domains.

5.5. 16PSH93: leucosome of the Lemu garnet-cordierite gneiss

Zircons from the Lemu leucosome are dark brown, translucent to transparent, mainly equidimensional and multifaceted. A few elongate grains also exist. Zircons are 200–400 μm long with a length/width ratios between 3.1 and 2:1. Some zircons have a turbid core domain and tiny inclusions are common. In BSE images, core domains and fractures with light alteration material are common, especially in the elongate zircons. The equidimensional zircons typically have a homogeneous internal structure (Fig. 2h).

Seven of the eight dated zircons give similar ages and one zircon gives an Archaean age. If the

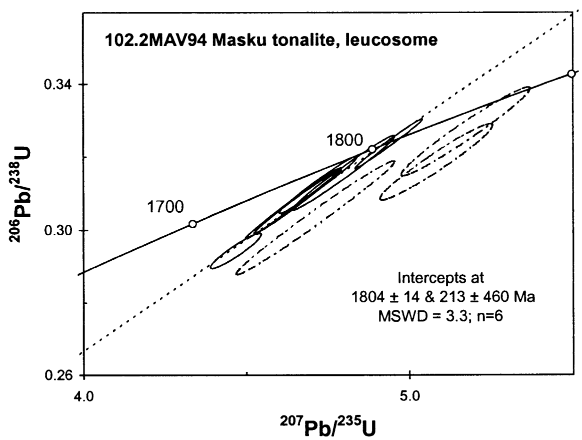

Fig. 6. Concordia plot for sample 102.2MAV94 Masku tonalite leucosome. Solid lines rims, dashed lines inherited cores.

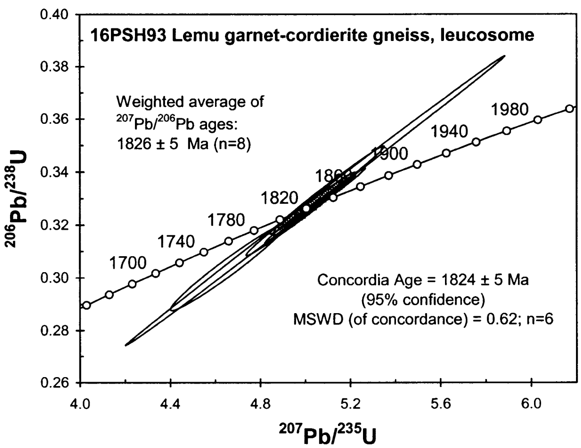

Fig. 7. Concordia plot for sample 16PSH94 Lemu garnet–cordierite gneiss leucosome.

youngest zircon from the mesosome material is added to the age calculations (see below), the weighted average of $^{207}Pb/^{206}Pb$ ages for the eight zircon spots is 1826 ± 5 Ma (MSWD $= 2.1$; $n = 8$). Leaving the mesosome zircon out, no intercept age can be calculated for these data, but the concordia age for the five concordant and one slightly discordant data points is 1824 ± 5Ma (MSWD $= 0.62$; $n = 6$; Fig. 7). This age determines well the age for migmatization.

5.6. 94MAV97: mesosome of the Lemu garnet–cordierite gneiss

The number of zircons obtained from the gneiss after separation was very small, only ten zircons. In addition, the zircon population is quite heterogeneous. The zircons are either equidimensional or elongate and they have clearly rounded facets. Their diameter range from 70 to 150 μm. One long grain with a length to width ratio of ≈ 3 also exists. In BSE images, almost all of the zircons show oscillatory zoning and some show clear core domains.

Because of the shortage of zircons and the heterogeneity of the zircon material only five spots were analyzed from this sample. Zircon number 01 has a zoned core domain with a $^{207}Pb/^{206}Pb$ age of 2.91 Ga surrounded by a narrow zoned new zircon phase with a probably mixed $^{207}Pb/^{206}Pb$ age of 2.38 Ga. Zircon number 10 gives the same age (≈ 1.98 Ga) from its core and the zoned major part of the grain. Elongate zircon number 06 gives a concordant age of 1.83 Ga that is identical to ages from the leucosome zircons. Therefore, it is considered that this zircon comes from the leucosome material.

6. Discussion

6.1. Age results

The tectonic setting of the Orijärvi granodiorite has been controversial. Latvalahti (1979) argued that the intrusive rocks in the middle of the volcanic belt are synorogenic and rose diapirically pushing earlier volcanic rocks aside. Colley and Westra (1987), based on field relationships and the similarity of geochemistry between intrusive and extrusive rocks, concluded that the intrusive rocks are pre-kinematic and cogenetic with volcanic rocks, i.e. they were magma chambers feeding volcanoes. Previous conventional U-Pb zircon dating of the granodiorite yielding the age of 1891 ± 13 Ma (Huhma, 1986), failed to distinguish between volcanic versus orogenic origin for the batholith. Published ages of both volcanic and orogenic igneous rocks are alike within errors (Patchett and Kouvo, 1986). The preferred intrusion age of 1898 ± 9 Ma now obtained in our new SIMS data has only marginally smaller errors than the previous conventional age. However, most of the zircons clearly show a magmatic growth zoning without any evidence of later metamorphic overgrowths, except for one with irregular core domain with slightly older apparent age (Fig. 2b). This older core might be an inherited relict from volcanic rocks below erosion surface, or it might represent earlier crystallised zircon within a long-lived magma chamber. Within errors, however, core and rim ages are the same. The obtained age still does not reveal the origin of the batholith because of the small differences between the volcanic and orogenic ages. Therefore, we made two conventional U-Pb zircon analyses from felsic volcanic rocks, one sample from the lowest stratigraphic level

(1895.3 ± 2.4 Ma) and another from the highest one (1878.2 ± 3.4 Ma). The results (Väisänen and Mänttäri, submitted) show that the sample from the Orijärvi batholith is coeval with the volcanic rocks, and the volcanite on the highest stratigraphic level is younger than the batholith, even with errors included. Therefore, as suggested by Colley and Westra (1987), the Orijärvi batholith is cogenetic with the volcanic rocks which it intruded.

The previous conventional U-Pb age of the synorogenic Masku hornblende tonalite at 1869 ± 5 Ma yields rather small uncertainties (Van Duin, 1992). However, BSE images and SIMS analyses indicate the existence of older Palaeoproterozoic and Archaean cores but no metamorphic overgrowth on the oscillatorily zoned zircons. Evidently, metamorphic temperatures at the amphibolite–granulite boundary (≈ 750 °C) were not enough to start a new metamorphic zircon growth. The new age (1854 ± 18 Ma) now obtained by SIMS has quite large errors, but combined with the conventional age of 1869 ± 5 Ma, 1.87 Ga or less can be considered as a true intrusion age. In addition, Nironen (1999) dated two synorogenic granitoids in adjacent area and obtained similar results (see Fig. 1). The inherited older Palaeoproterozoic and Archaean cores clearly indicate incorporation of older crustal material in the samples. Patchett and Kouvo (1986) also pointed out, that ε_{Nd} values in trondhjemites in southern Finland suggest a minor older crustal precursor to some of the igneous rocks. However, there is too little data to argue whether older material was incorporated by assimilation (cf. Nironen, 1997) or sediment-derived zircons (cf. Claesson et al., 1993).

The Kakskerta enderbite is situated within the Turku low pressure/high temperature granulites that reached temperatures of 800 °C or more (Väisänen and Hölttä, 1999). The spatial connection between granulites and enderbites combined with conventional U-Pb zircon ages led Van Duin (1992) to propose that the intrusions were responsible for the granulite facies metamorphism. Väisänen and Hölttä (1999), however, challenged this idea and argued, on a structural basis, that enderbites were already deformed by D2 while the peak metamorphism took place some 30 Ma later during D3. Suominen (1991) analyzed the same sample used in this study and obtained two ages on different types of zircons, 1880 and 1840 Ma. The zircons analyzed in this study showed very complex age patterns. The core ages (1874 ± 54 Ma) from the zoned zircons, as well as the concordant rim ages of 1876 ± 5 Ma together are inferred to represent the intrusion age of 1878 ± 19 Ma, while the ≈ 1.82 Ga ages from the zoned rims and recrystallized cores are interpreted as metamorphic overgrowths. The youngest ≈ 1750 Ma core age must represent metamict lead loss at that time. In summary, the field observations (Väisänen and Hölttä, 1999) and SIMS data indicate that the Kakskerta enderbite belongs to the synorogenic intrusive suite that has been metamorphosed during granulite facies metamorphism resulting in new zircon growth. Previous, heterogeneous conventional U-Pb zircon datings were a result of mixture of at least two generations of zircons.

The patchy leucosome of the Masku tonalite yielded an age of 1804 ± 14 Ma. One of the analysis was concordant and yielded an age of 1810 ± 4 suggesting that the age of migmatization is closer to the older than the younger end of the error limits. Within error limits, these analyses agree with the conventional U-Pb zircon age of 1814.3 ± 2.7 Ma obtained from a garnet-bearing, S-type, anatectic granite in the same area (Väisänen et al., 2000). The other leucosome sample was from a garnet- and cordierite-bearing leucosome intruding along the axial plane of regional F3 folding. The age of 1824 ± 5 Ma from this sample accurately determines the age of regional anatexis. Since the leucosome fills F3 fold hinges and intrudes their axial planes, it also constrains the age of F3 folding (Väisänen and Hölttä, 1999). The garnet–cordierite gneiss mesosome sample contained strongly abraded detrital zircons and four analyses yielded $^{207}Pb/^{206}Pb$ ages of 2.91, 2.38, 1.98 and 1.98 Ga. These ages are in accordance with ages obtained by the SHRIMP method from detrital zircons from Orijärvi, 100 km to the east (Claesson et al., 1993). One euhedral elongate zircon yielded an $^{207}Pb/^{206}Pb$ age of 1829 ± 6, i.e. the same age as in the leucosome sample. It was probably derived from the tiny leucosome stripes present in the sample. The absence of island-arc-related detrital zircons (1.90–1.88 Ga) indicate that the sedimentary material came outside the local volcanic arcs, which may have been subaqueous and incapable of producing erosional detritus. In summary, the leucosome samples provide the age of anatexis and the peak metamorphism. Anatexis began at ≈ 1.83 Ga and continued at least until ≈ 1.81 Ga, possibly to 1.80 Ga. These ages are in accordance with the metamorphic zircon ages from the Kakskerta enderbite. It is noteworthy that no metamorphism predating the granulite facies was detected in the samples. Using the timing of metamorphic mineral growth in relation to structures, Väisänen and Hölttä (1999) concluded that crystallization of garnet and cordierite and the onset of melting began before D3 deformation. However, this could not be verified in this study. Perhaps pre-existing zircons were totally dissolved to produce new zircons detected in this study, or alternatively, the temperature of the previous metamorphism was not high enough to produce zircons. 100 km southeast of the present study area, Hopgood et al. (1983) report U-Pb ages of 1.88–1.87 Ga derived from monazites in garnet-bearing gneiss and aplitic veins. They interpret these as metamorphic ages. Together with 1.88–1.86 Ga ages of synorogenic intrusions, this suggests that metamorphism of that age also took place in southernmost Finland.

6.2. Regional implications

The geological history of the Southern Svecofennian Arc Complex (SSAC) differs in many ways from the geology of the Central Svecofennian Granitoid Complex (CSAC). Northeast of the CFGC (Fig. 1) peak metamorphism was coeval with intrusion of 1885 Ma enderbites (Hölttä, 1995). Peak metamorphism at the southern margin of the CFGC in the Tampere Schist Belt is now determined at 1878.5 ± 1.5 Ma (Mouri et al., 1999), coeval with 1.88 Ga collision-related magmatism. Soon after the collision, crust was stabilized at 1.88–1.87 Ga when post-kinematic, bimodal, magmatism took place (Nironen et al., 2000).

In the SSAC the earliest intrusive magmatism (1.91–1.88 Ga) is coeval with volcanism. This belongs to the original idea of Hietanen (1975) of an island–arc origin for Svecofennian formations. It is often difficult to know whether intrusions are arc- or orogen-related. Unequivocal crosscutting field relationships or accurate age determinations are needed. Early orogenic magmatism, dated at 1.88–1.86 Ga, is ≈ 10 Ma younger in the SSAC than in the CSAC and is coeval with post-kinematic magmatism in that area. Therefore, these two areas do not share a common tectonic evolution, and the idea of a suture zone between these areas (Lahtinen, 1996) is supported. Collision of the SSAC with the CSAC probably took place at 1.88–1.86, i.e. ≈ 10–20 Ma later than the collision of the CSAC arc with the Archaean craton.

The high heat flow that produced granulite facies metamorphism is restricted to the LSGM. Peak metamorphism that triggered crustal anatexis started at 1.84–1.83 Ga as indicated by zircon growth in enderbites and leucosomes within the granulite area. Melt formation continued 20–30 Ma to 1.81 Ga, probably because continued mafic, mantle derived magmatism provided additional heat during that time period. Väisänen et al. (2000) suggested that convective removal of the subcontinental lithospheric mantle during upwelling asthenosphere caused melting of the enriched parts of the mantle under this part of the Fennoscandian Shield during post-collisional stage. These were intruded into the middle crust causing the post-collisional high grade metamorphism.

7. Conclusions

From the ion microprobe (SIMS) dating of zircons, we draw the following conclusions:

1. The Orijärvi granodiorite belongs to the 1.91–1.88 Ga arc magmatism.
2. Synorogenic magmatism is dated at 1.88–1.86 Ga, i.e. 10 Ma younger than related magmatism in the Central Finland Granitoid Complex and Tampere Schist Belt.
3. Collision-related D2 deformation is ≤ 1.87 Ga in age.

4. Peak metamorphism took place at 1824 ± 5 Ma in the Turku area. This also dates the age of the D3 folding. Crustal melting continued until at least 1.81 Ga.
5. Zircons in the synorogenic ≈ 1.88–1.86 Ga Kakskerta enderbite obtained a new metamorphic overgrowth in the Turku granulite area, but the coeval zircons in tonalite in the amphibolite–granulite boundary area were not affected.
6. Some zircons in the synorogenic Masku intrusion contain older Palaeoproterozoic and Archaean cores.
7. Sedimentary detritus in metapelites came outside the local volcanic arcs.

Acknowledgements

Many thanks are owed to Hannu Huhma for providing samples A498 and A933 for our use. The helpful assistance of the staff in the Nordsim laboratory, Kerstin Lindén, Torbjörn Sunde, Jessica Vestin and Martin Whitehouse are greatly acknowledged. Paul Evins and Dmitry Konopelko reviewed the early version of the manuscript and both are acknowledged. J.D. Kramers and Torbjörn Skiöld reviewed and suggested many valuable improvements to the manuscript. This study was funded by the Lithosphere Graduate School and the Academy of Finland (project No. 40553). This is NORDSIM contribution number 60.

References

Claesson, S., Huhma, H., Kinny, P.D., Williams, I.S., 1993. Svecofennian detrital zircon ages—implications for the Precambrian evolution of the Baltic Shield. Precambrian Res. 64, 109–130.

Colley, H., Westra, L., 1987. The volcano–tectonic setting and mineralisation of the early Proterozoic Kemiö–Orijärvi–Lohja belt, SW Finland. In: Pharaoh, T.C., Beckinsale, R.D., Rickard, D. (Eds.), Geochemistry and Mineralisations of Proterozoic Volcanic Suites, vol. 33. Blackwell: Geological Society of London Special Publications, Oxford, pp. 95–107.

Ehlers, C., Lindroos, A., Selonen, O., 1993. The late Svecofennian granite–migmatite zone of southern Finland—a belt of transpressive deformation and granite emplacement. Precambrian Res. 64, 295–309.

Eklund, O., Konopelko, D., Rutanen, H., Fröjdö, S., Shebanov, A.D., 1998. 1.8 Ga Svecofennian post-collisional shoshonitic magmatism in the Fennoscandian shield. Lithos 45, 87–108.

Gaál, G., Gorbatchev, R., 1987. An outline of the Precambrian evolution of the Baltic shield. Precambrian Res. 35, 15–52.

Haudenschild, U., 1995. The Vaaraslahti pyroxene granitoid intrusion and its contact aureole: isotope geology. Geol. Surv. Finland Bull. 382, 81–89.

Hietanen, A., 1947. Archaean geology of the Turku district in southwestern Finland. Bull. Geol. Soc. Am. 58, 1019–1084.

Hietanen, A., 1975. Generation of potassium-poor magmas in the northern Sierra Nevada and the Svecofennian in Finland. J. Res. US Geol. Surv. 3, 631–645.

Hölttä, P., 1995. Contact metamorphism of the Vaaraslahti pyroxene granitoid intrusion in Pielavesi, Central Finland. Geol. Surv. Finland Bull. 382, 27–79.

Hopgood, A.M., Bowes, D.R., Kouvo, O., Halliday, A.D., 1983. U-Pb and Rb-Sr isotopic study of polyphase deformed migmatites in the Svecokarelides, southern Finland. In: Atherton, M.P., Gribble, C.D. (Eds.), Migmatites, Melting and Metamorphism. Shiva, Nantwich, pp. 80–92.

Huhma, H., 1986. Sm–Nd, U-Pb and Pb–Pb isotopic evidence for the origin of the early Proterozoic Svecokarelian crust in Finland. Geol. Surv. Finland Bull. 337, 48p.

Kähkönen, Y., Huhma, H., Aro, K., 1989. U-Pb zircon ages and Rb–Sr whole rock isotope studies of early Proterozoic volcanic and plutonic rocks near Tampere, southern Finland. Precambrian Res. 45, 27–43.

Kilpeläinen, T., 1998. Evolution and 3D modelling of the structural and metamorphic patterns of the Palaeproterozoic crust in the Tampere-Vammala area, southern Finland. Geol. Surv. Finland Bull. 397, 124p.

Kontinen, A., 1987. An early Proterozoic ophiolite—the Jormua mafic–ultramafic complex, northeastern Finland. Precambrian Res. 35, 313–341.

Korja, A., Korja, T., Luosto, U., Heikkinen, P., 1993. Seismic and geoelectric evidence for collisional and extensional events in the Fennoscandian Shield—implications for Precambrian crustal evolution. Tectonophysics 219, 129–152.

Korsman, K., Hölttä, P., Hautala, T., Wasenius, P., 1984. Metamorphism as an indicator of evolution and structure of crust in Eastern Finland. Geol. Surv. Finland Bull. 328, 40p.

Korsman, K., Koistinen, T., Kohonen, J., Wennerström, M., Ekdahl, E., Honkamo, M., Idman, H., Pekkala, Y. (Eds.) 1997. Bedrock Map of Finland 1:1000 000. Geological Survey of Finland, Espoo, Finland.

GGTS/VEKA Working Group, Korsman, K., Korja, T., Pajunen, M., Virransalo, P., 1999. The GGT/SVEKA transect: structure and evolution of the continental in the Paleoproterozoic Svecofennian Orogen in Finland. Internat. Geol. Rev. 41, 287–333.

Kouvo, O., 1958. Radioactive age of some Finnish pre-Cambrian minerals. Bull. Comm. Géol. Finlande 182, 70p.

Kouvo, O., Tilton, G.R., 1966. Mineral ages from the Finnish Precambrian. J. Geol. 74, 421–442.

Lahtinen, R., 1994. Crustal evolution of the Svecofennian and Karelian domains during 2.1–1.79 Ga, with special emphasis on the geochemistry and origin of 1.93–1.91 Ga gneissic tonalites and associated supracrustal rocks in the Rautalampi area, central Finland. Geol. Surv. Finland Bull. 378, 128p.

Lahtinen, R., 1996. Geochemistry of Palaeproterozoic supracrustal and plutonic rocks in the Tampere–Hämeenlinna area, southern Finland. Geol. Surv. Finland Bull. 389, 113p.

Latvalahti, U., 1979. Cu–Pb–Zn ores in the Aijala–Orijärvi area, Southwest Finland. Econ. Geol. 74, 1035–1059.

Lee, J.K.W., Williams, I.S., Ellis, D.J., 1997. Pb, U and Th diffusion in natural zircons. Nature 390, 159–161.

Lindberg, B., Bergman, L., 1993. Pre-Quaternary rocks of the Vehmaa map-sheet area. Geological map of Finland 1:100 000. Explanation to the maps of Pre-Quaternary rocks, sheet 1042. Geological Survey of Finland, Espoo, 56 p.

Ludvig, K.R., 1998. Isoplot/Ex Version 1.00. Berkeley Geochronological Center, Special Publication 1, 43 p.

Mezger, K., Krogstad, E.J., 1997. Interpretation of discordant U-Pb zircon ages; an evaluation. J. Metamorph. Geol. 15, 127–140.

Mouri, H., Korsman, K., Huhma, H., 1999. Tectono–metamorphic evolution and timing of the melting processes in the Svecofennian Tonalite–Trondhjemite Migmatite belt: an example from Luopioinen, Tampere area, southern Finland. Bull. Geol. Soc. Finland 71, 31–56.

Nironen, M., 1989. Emplacement and structural setting of granitoids in the early Proterozoic Tampere and Savo Schist Belts, Finland—implications for contrasting crustal evolution. Geol. Surv. Finland Bull. 346, 83p.

Nironen, M., 1997. The Svecofennian Orogen: a tectonic model. Precambrian Res. 86, 21–44.

Nironen, M., 1999. Structural and magmatic evolution in the Loimaa area, southwestern Finland. Bull. Geol. Soc. Finland 71, 57–71.

Nironen, M., Elliott, B.A., Rämö, O.T., 2000. 1.88–187 Ga post-kinematic intrusions of the Central Finland Granitoid Complex: a shift from C-type to A-type magmatism during lithospheric convergence. Lithos 53, 37–58.

Patchett, J., Kouvo, O., 1986. Origin of continental crust of 1.9–1.7 Ga age: Nd isotopes and U-Pb zircon ages in the Svecokarelian terrain of South Finland. Contr. Mineral. Petrol. 92, 1–12.

Ploegsma, M., Westra, L., 1990. The early Proterozoic Orijärvi triangle (southwest Finland): a key area on the tectonic evolution of the Svecofennides. Precambrian Res. 47, 51–69.

Schreurs, J., Westra, L., 1986. The thermotectonic evolution of a Proterozoic, low pressure, granulite dome, West Uusimaa, SW Finland. Contribut. Mineral. Petrol. 93, 236–250.

Stacey, J.S., Kramers, J.D., 1975. Approximation of terrestrial lead isotope evolution by a two-stage model. Earth Planet. Sci. Letts. 26, 207–221.

Suominen, V., 1991. The chronostratigraphy of southwestern Finland with special reference to Postjotnian and Subjotnian diabases. Geol. Surv. Finland Bull. 356, 100p.

Vaasjoki, M., 1977. Rapakivi granites and other postorogenic rocks in Finland: their age and the lead isotopic composition of certain associated galena mineralizations. Geol. Surv. Finland Bull. 294, 64p.

Vaasjoki, M., 1996. Explanation to the geochronological map of southern Finland: The development of the continental crust with special reference to the Svecofennian orogeny. Geol. Surv. Finland Rep. Invest. 135, 30p.

Vaasjoki, M., Sakko, M., 1988. The evolution of the Raahe–Ladoga zone in Finland: isotopic constraints. Geol. Surv. Finland Bull. 343, 7–32.

Väisänen, M., Hölttä, P., 1999. Structural and metamorphic evolution of the Turku migmatite complex, southwestern Finland. Bull. Geol. Soc. Finland 71, 177–218.

Väisänen M., Mänttäri I., 2002. U-Pb ages and tectonic setting of volcanic formations in the Orijärvi area, southwestern Finland. In: Korkka-Niemi, K. (ed.) Geologian tutkijapäivät, Helsinki 13–14.3.2002, Abstracts, 9–10.

Väisänen, M., Mänttäri, I., Kriegsman, L.M., Hölttä, P., 2000. Tectonic setting of post-collisional magmatism in the Palaeoproterozoic Svecofennian Orogen, SW Finland. Lithos 54, 63–81.

Van Duin, J.A., 1992. The Turku granulite area, SW Finland: a fluid-absent Svecofennian granulite occurrence. Academisch Proefschrift. Vrije Universiteit, Amsterdam. PhD thesis, 234 p.

Wetherill, G., Kouvo, O., Tilton, G., Gast, P., 1962. Age measurements of rocks from the Finnish Precambrian. J. Geol. 70, 74–88.

Whitehouse, M.J., Claesson, S., Sunde, T., Vestin, J., 1997. Ion microprobe U-Pb zircon geochronology and correlation of Archean gneisses from the Lewisian Complex of Gruinard Bay, northwestern Scotland. Geochim. Cosmochim. Acta 61, 4429–4438.

Whitehouse, M.J., Kamber, B., Moorbath, S., 1999. Age significance of U–Th–Pb zircon data from early Archaean rocks of west Greenland—a reassessment based on combined ion-microprobe and imaging studies. Chem. Geol. 160, 201–224.

Wiedenbeck, M., Allé, P., Corfu, F., Griffin, W.L., Meier, M., Oberli, F., von Quadt, A., Roddick, J.C., Spiegeln, W., 1995. Three natural zircon standards for U–Th–Pb, Lu–Hf, trace element and REE analysis. Geostand. Newslett. 19, 1–23.

Williams, I.S., 1998. U–Th–Ub geochronology by ion microprobe. Rev. Econ. Geol. 7, 1–35.